Double-Input DC–DC Power Electronic Converters for Electric-Drive Vehicles—Topology Exploration and Synthesis Using a Single-Pole Triple-Throw Switch

Karteek Gummi and Mehdi Ferdowsi, *Member, IEEE*

***Abstract*—Hybridizing energy systems using storage devices has gained popularity in transportation and distributed electric power generation applications. Traditionally, several independent power electronic converters (PECs) were utilized in such practices. Due to their reduced part count, double-input (DI) PECs prove to be a promising choice in hybridizing energy systems. A few topologies for multi-input converters have been reported in the literature; however, there is no systematic approach to synthesize them. Furthermore, all possible topologies are not completely explored, and it is difficult to derive new converters from existing topologies. Therefore, in this paper, a systematic approach to derive DI converters by using a single-pole triple-throw switch as a building block is presented.**

***Index Terms*—DC–DC power conversion, energy storage, multiport converters.**

I. Introduction

DOUBLE-INPUT (DI) converters have gained popularity in power electronic applications including electric, hybrid, and plug-in hybrid electric vehicles; fuel cell systems; photovoltaic systems [1], [2]; wind generation [3], [4]; and power factor correction [5]. In these applications, utilizing a short- or long-term energy storage device is inevitable since the instantaneous values of the input and output powers are not equal [6]–[11]. The energy storage unit can be comprised of batteries and/or electrochemical capacitors. In other words, the storage unit can be hybridized itself.

Electrochemical capacitors have been proposed to be utilized in the electrical distribution system of conventional and hybrid vehicles to serve applications like local energy cache, voltage smoothing, pseudo-42-V architecture, and service life of batteries extension. However, the high specific power of electrochemical capacitors is the major reason for having them used as an intermediate energy storage unit during acceleration, hill climbing, and regenerative braking. A hybrid energy storage unit comprising both batteries and electrochemical capacitors seems to be the promising choice for future electric drive vehicles. The basic idea is to realize the advantages of both batteries and electrochemical capacitors while keeping the weight of the entire energy storage unit minimized through an appropriate matching.

In order to combine the main source of power with the energy storage unit or in order to hybridize the energy storage unit, either two independent converters or a single DI converter is needed. The advantages of using a DI converter include reduced component count, lower cost, and control simplicity. These advantages can potentially improve the overall cost and efficiency of electric drive vehicles.

Magnetic coupling has been used to develop DI and, more generally, multi-input converters [12]–[17]. Combining the structure of independent power converters has also been proposed to make multiport converters [18]–[22]. These approaches do not systematically use building blocks to derive DI power electronic converters (DIPECs). Furthermore, all possible topologies have not been completely explored. In addition, it is difficult to derive new DI converters using existing DI topologies. Hence, in this paper, a single-pole triple-throw (SPTT) switch is used as a building block in creating DIPECs.

Three DI dc–dc converters are proposed in Section II. The operating modes of the new converters, as well as their voltage transfer ratios in the continuous conduction mode, are also described. In Section III, the switch realization of the converters is discussed. Simulation and experimental results to verify the converters' characteristics are presented in Sections IV and V, respectively. Finally, Section VI draws the concluding remarks.

II. Derivation of New DI Converters Using an SPTT Switch

Fig. 1 shows a simple representation of an SPTT switch. At any given time, the pole is connected to one and only one of the throws. An SPTT switch can be realized by using three single-pole single-throw (SPST) switches, as shown in Fig. 2. It should be reminded that one and only one of the three SPST switches is on at any given time [23].

Manuscript received March 10, 2009; revised September 8, 2009. First published September 22, 2009; current version published January 13, 2010. This work was supported in part by the National Science Foundation under Grant 0640636.

K. Gummi is with the Bechtel Corporation, Houston, TX 77056-6580 USA (e-mail: kgummi@bechtel.com).

M. Ferdowsi is with the Department of Electrical and Computer Engineering, Missouri University of Science and Technology, Rolla, MO 65409 USA (e-mail: ferdowsi@mst.edu).

Color versions of one or more of the figures in this paper are available online at http://ieeexplore.ieee.org.

Digital Object Identifier 10.1109/TIE.2009.2032762

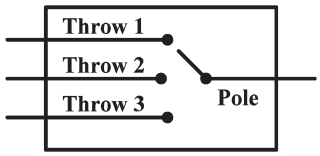

Fig. 1. SPTT switch.

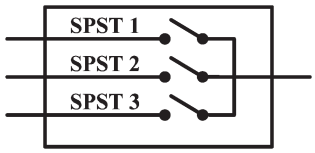

Fig. 2. SPTT switch realized using three SPST switches.

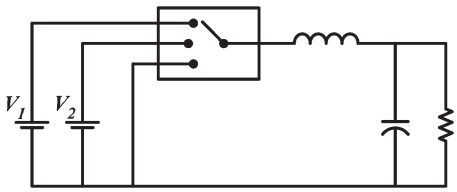

Fig. 3. DI buck converter using an SPTT switch.

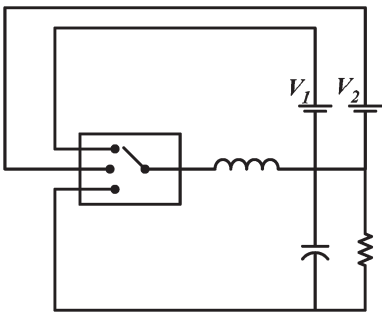

Fig. 4. DI buckboost converter using an SPTT switch.

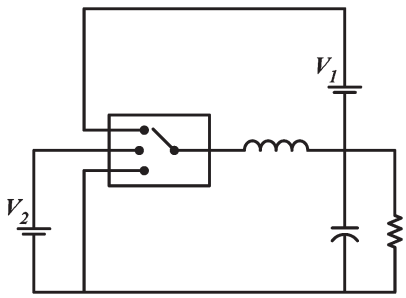

Fig. 5. DI buckboost-buck converter using an SPTT switch.

Figs. 3–5 show the circuit diagrams of the new DIPECs that can be synthesized using an SPTT switch. Here, these converters are named DI buck, DI buckboost, and DI buckboost-buck topologies, respectively. Although voltage sources are used for the graphic demonstration of these topologies, any stiff dc voltage source or storage mechanism can be used. It is worth mentioning that only one inductor is used in the structure of these converters. Therefore, they benefit from a higher power density. These converters are derived and will be analyzed using basic PEC topologies reported in the literature [12], [13], [19]–[21], [24]–[28]. Similar to classic power electronic approaches, parasitic components will be neglected in the analysis.

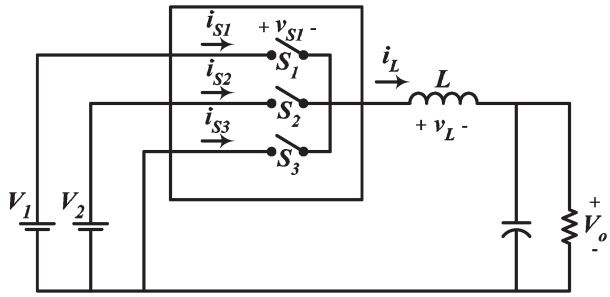

Fig. 6. DI buck converter using three SPST switches.

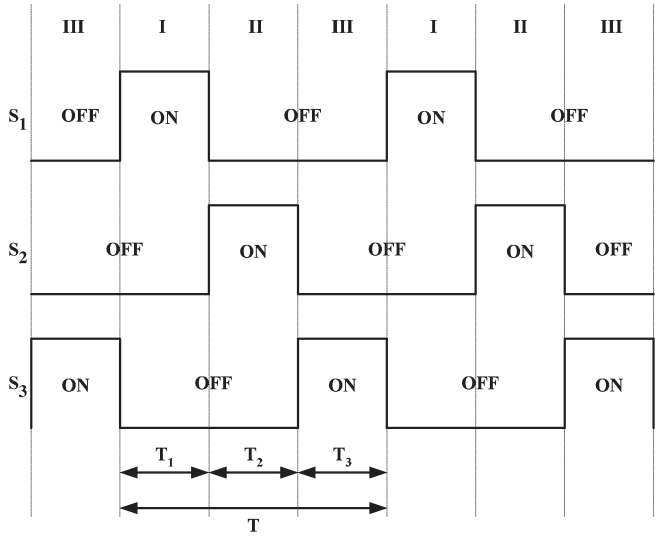

Fig. 7. Switching patterns of a DI buck converter.

TABLE I
VOLTAGE ACROSS INDUCTOR FOR DIFFERENT MODES OF OPERATION OF DI BUCK CONVERTER

Mode	ON Switch	V_L	Note
I	S_1	V_1 - V_o	V_1 supplies energy
II	S_2	V_2 - V_o	V_2 supplies energy
III	S_3	- V_o	Freewheeling

Fig. 6 shows the circuit diagram of the DI buck converter using three SPST switches instead of one SPTT switch. This replacement makes the switch realization easier. Voltage source V_1 delivers power when SPST switch S_1 is turned on. Similarly, voltage source V_2 is the source of power when switch S_2 is on. Finally, switch S_3 can be used for freewheeling purposes. Fig. 7 shows a typical switching pattern for the three SPST switches. This pattern can be applied to any of the DIPECs discussed here. Three modes of operation for a DI buck converter that occur under unidirectional power flow are described in Table I. Similarly, the modes of operation for the DI buckboost and buckboost-buck converters are shown in Tables II and III, respectively. It is worth mentioning that Mode III does not have to appear at the end of the switching period. All or parts of it can be placed between Modes I and II.

TABLE II
VOLTAGE ACROSS INDUCTOR FOR DIFFERENT MODES OF OPERATION OF DI BUCKBOOST CONVERTER

Mode	ON Switch	V_L	Note
I	S_1	V_1	V_1 supplies energy
II	S_2	V_2	V_2 supplies energy
III	S_3	$-V_o$	Freewheeling

TABLE III
VOLTAGE ACROSS INDUCTOR FOR DIFFERENT MODES OF OPERATION OF DI BUCKBOOST-BUCK CONVERTER

Mode	ON Switch	V_L	Note
I	S_1	V_1	V_1 supplies energy
II	S_2	$V_2 - V_o$	V_2 supplies energy
III	S_3	$-V_o$	Freewheeling

One can observe in Fig. 7 that T_1 is the on-time of switch S_1, T_2 is the on-time of switch S_2, and T_3 is the on-time of switch S_3. Hence

$$T_1 = d_1 * T \quad T_2 = d_2 * T \quad T_3 = d_3 * T \tag{1}$$

$$T_1 + T_2 + T_3 = T \tag{2}$$

where T is the switching period and d_1, d_2, and d_3 are the duty cycles of switches S_1, S_2, and S_3, respectively. Considering a DI buck converter, one can write the following equation based on Fig. 7, Table I, and the volt–second balance equation of the inductor:

$$T_1 * (V_1 - V_O) + T_2 * (V_2 - V_O) + T_3(-V_O) = 0. \tag{3}$$

This can be simplified to the following equation:

$$V_1 * T_1 + V_2 * T_2 = V_O * (T_1 + T_2 + T_3). \tag{4}$$

Combining (1), (2), and (4), one can obtain the following equation which describes the relation between the input and output voltages:

$$V_O = d_1 * V_1 + d_2 * V_2. \tag{5}$$

Similarly, voltage transfer ratios of the DI buckboost and buckboost-buck converters can be described as

$$V_O = \frac{d_1}{1 - d_1 - d_2} * V_1 + \frac{d_2}{1 - d_1 - d_2} * V_2 \tag{6}$$

$$V_O = \frac{d_1}{1 - d_1} * V_1 + \frac{d_2}{1 - d_1} * V_2. \tag{7}$$

In employing (5)–(7), one should keep in mind that

$$d_1 + d_2 \leq 1. \tag{8}$$

For instance, in a DI buck converter, (8) indicates that V_o cannot exceed $\text{Max}(V_1, V_2)$. Variations of the output voltage as a function of the duty ratios for a DI buck converter are shown in Fig. 8. In this figure, V_1 and V_2 are selected to be 80 and 60 V, respectively.

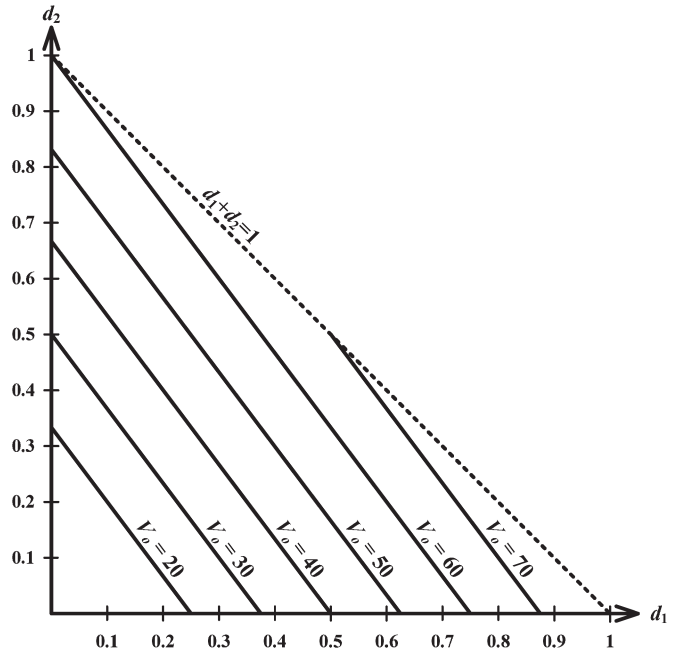

Fig. 8. Variations of the output voltage in a DI buck converter as a function of the duty ratios when $V_1 = 80$ V and $V_2 = 60$ V.

III. SWITCH REALIZATION FOR NEW DI CONVERTER TOPOLOGIES

In the DI buck converter shown in Fig. 6, SPST switches S_1, S_2, and S_3 can be realized using diodes and transistors. Switch realization depends on the input and output voltage levels as well as the power flow direction. Assuming that the power flow is from left to right (or $i_L > 0$), one can argue

$$\begin{aligned}
&(\text{If } S_1 \text{ is on} \rightarrow S_2 \text{ and } S_3 \text{ are off})\\
&\quad => (i_{S1} > 0, V_{S2} = V_2 - V_1, \text{ and } V_{S3} = -V_1)\\
&(\text{If } S_2 \text{ is on } \rightarrow S_1 \text{ and } S_3 \text{ are off})\\
&\quad => (i_{S2} > 0, V_{S1} = V_1 - V_2, \text{ and } V_{S3} = -V_2)\\
&(\text{If } S_3 \text{ is on } \rightarrow S_1 \text{ and } S_2 \text{ are off})\\
&\quad => (i_{S3} > 0, V_{S1} = V_1, \text{ and } V_{S2} = V_2).
\end{aligned}$$

Therefore, SPST switch S_1 conducts positive currents and has to block either a positive or a negative voltage depending on the magnitude of V_1 and V_2. Consequently, it should be replaced by a diode in series with a transistor. Similarly, switch S_2 should be a bidirectional voltage blocking switch. Switch S_3, which conducts positive currents and opposes negative voltages, should be replaced by a diode. Therefore, the final circuit diagram of the DI buck converter is shown in Fig. 9.

The structure of a DI buck converter can be simplified to Fig. 10 if V_1 is always greater than V_2 $(V_1 > V_2)$. Similarly, the structure of the DI buck converter can be further simplified if V_1 is always greater than V_2 $(V_1 > V_2)$ and Mode III never

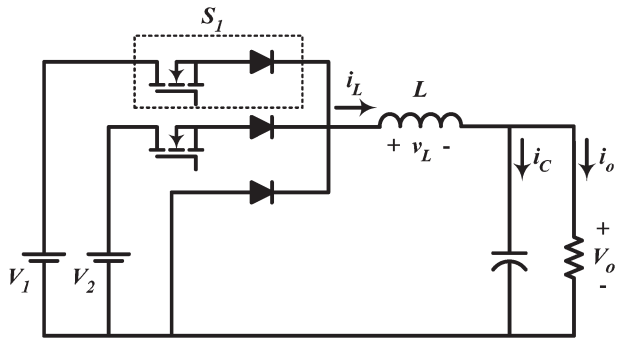

Fig. 9. Switch realization for the DI buck converter (unidirectional power flow).

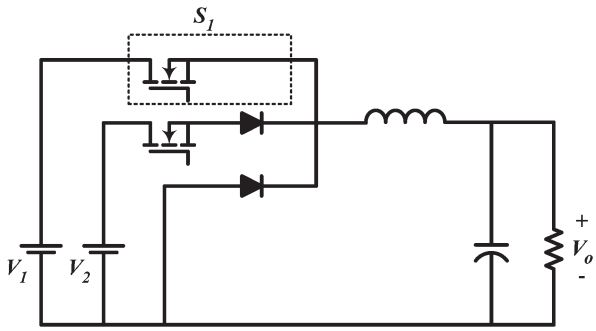

Fig. 10. Simplified DI buck converter (if $V_1 > V_2$).

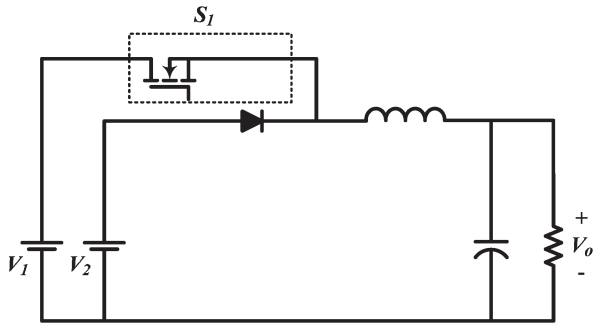

Fig. 11. Further simplified DI buck converter with $V_1 > V_2$ and no Mode III.

occurs. The simplified converter in this case is shown in Fig. 11. This converter is similar to a two-input buck converter [5].

Similarly, the unidirectional switch realization for the DI buckboost and buckboost-buck converters results in the final circuits shown in Figs. 12 and 13, respectively. These two topologies may also be further simplified similar to the discussion presented for the DI buck converter.

In applications such as hybrid electric vehicles and photovoltaic systems, one of the dc sources noted by V_1 or V_2 is a battery. Hence, bidirectional power flow to and from one of the sources (V_1 in this paper) is required. In this case, switch realization will be slightly different

$$(\text{If } S_1 \text{is on}) => (i_{S1} > 0 \text{ or } < 0)$$

$$(\text{If } S_2 \text{ is on} \rightarrow S_1 \text{ is off}) => (V_{S1} > 0 \text{ or } < 0).$$

As switch S_1 conducts either a positive or a negative current and also blocks either a positive or a negative voltage, it must be replaced by a four-quadrant switch (see Fig. 14).

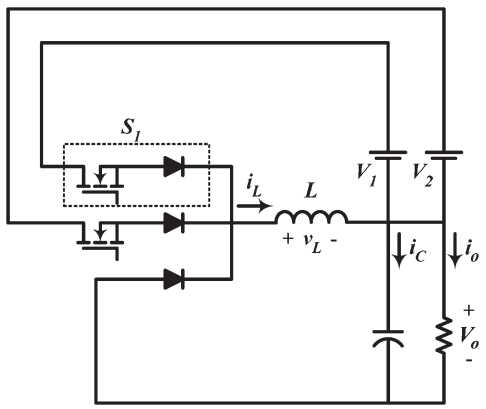

Fig. 12. Switch realization for the DI buckboost converter (unidirectional power flow).

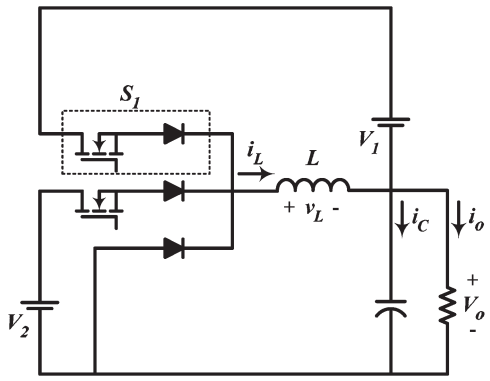

Fig. 13. Switch realization for the DI buckboost-buck converter (unidirectional power flow).

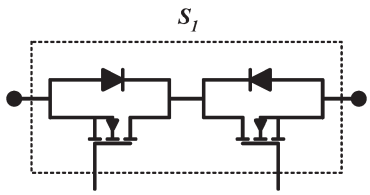

Fig. 14. Four-quadrant switch for bidirectional power flow.

IV. Simulation Results

Figs. 15–17 show the simulation results of the DI buck, buckboost, and buckboost-buck converters, respectively. Two dc voltage sources $V_1 = 100$ V and $V_2 = 150$ V are used as input voltage sources. The switching commands for S_1 and S_2 have fixed duty ratios of 0.3 and 0.4 at the switching frequency is 100 kHz. The inductor value was selected to be 200 μH, the capacitor value was 80 μF, and the load resistance was 5 Ω. From top to bottom are the waveforms of the switch commands for S_1 and S_2, inductor voltage V_L, inductor current i_L, and the output voltage. One can observe from the waveforms that the average value of the output voltage for the DI buck converter is 90 V. This can also be obtained from the voltage transfer ratio described in (5). Similarly, the output voltages of the DI buckboost and buckboost-buck converters are regulated at 300 and 128.6 V, which can also be obtained by (6) and (7), respectively.

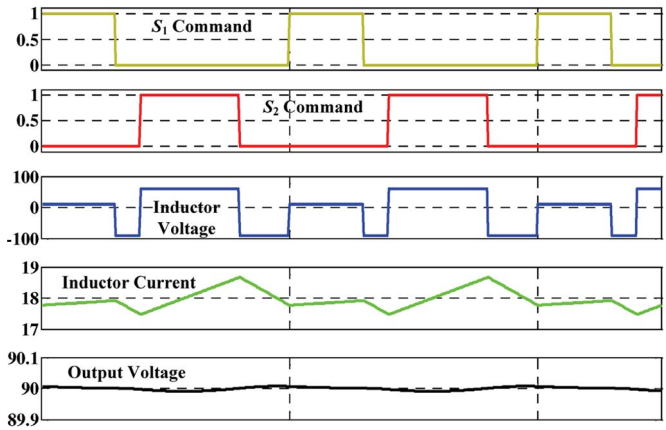

Fig. 15. Simulation results of the DI buck converter.

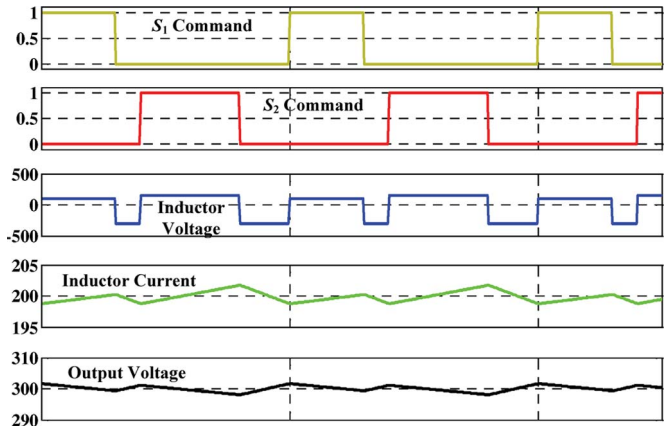

Fig. 16. Simulation results of the DI buckboost converter.

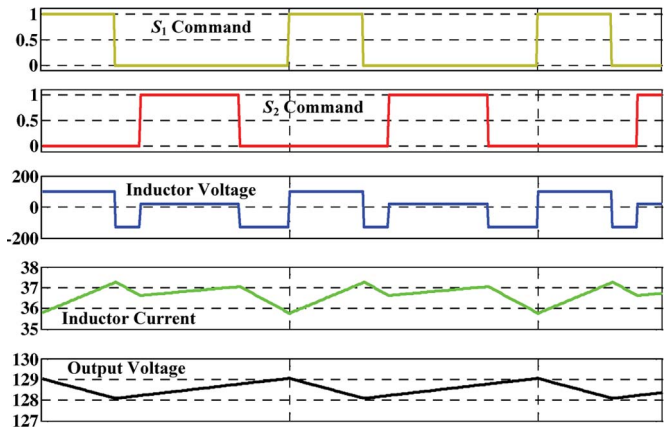

Fig. 17. Simulation results of the DI buckboost-buck converter.

The peak-to-peak ripple of the inductor current in a DI buck converter is at its maximum level when $V_1 = V_2$ and Mode II occurs right after Mode I. Similar to a single-input buck converter, in order to make sure that the converter operates in the continuous conduction mode, one needs to make sure that the inductor value is greater than

$$L_{\text{Critical}} = \frac{R(1-d_1-d_2)}{2f_s} \tag{9}$$

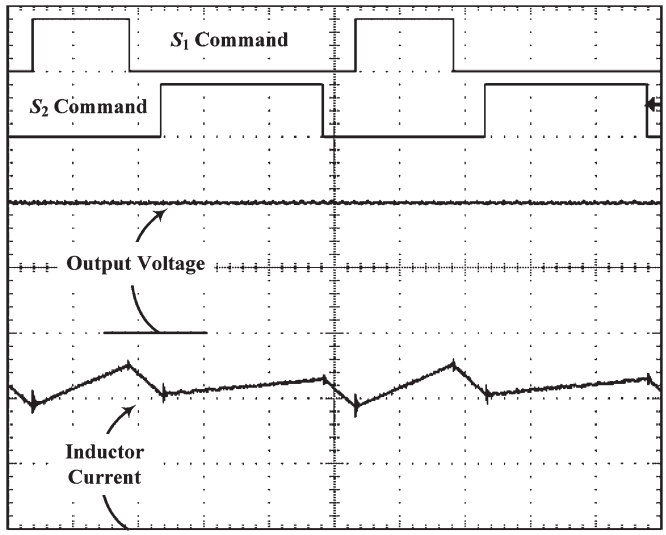

Fig. 18. Experimental output voltage and inductor current waveforms of a DI buck converter (voltage: 25 V/div, current: 5 A/div, and time: 4 μs).

where R is the load resistance and f_s is the switching frequency. Similarly, under the same conditions, one can describe the peak-to-peak ripple of the output voltage in a DI buck converter as [29]

$$\frac{\Delta v_o}{V_o} = \frac{1-d_1-d_2}{8LCf_s^2} \tag{10}$$

where ΔV_o is the peak-to-peak ripple of the output voltage and C is the output capacitor.

V. Experimental Verification

In order to verify the simulation results, a low-power laboratory prototype of a DI buck converter was built. Sources V_1 and V_2 were selected to be 80- and 60-V power supplies. Dual-pack IGBT switches were used for S_1 and S_2. The switching frequency was 50 kHz. A 50-μH inductor and a 150-μF capacitor were used as L and C, respectively. The load resistance was about 4.5 Ω, and the output power was expected to be around 550 W.

Duty cycles d_1 and d_2 were selected to be 0.3 and 0.5, respectively. Mode II does not start immediately after Mode I. Mode III is placed before and after Mode II. The open-loop results are shown in Figs. 18 and 19. Fig. 18 contains the waveforms of output voltage V_o and inductor current i_L. When both switches are off, the inductor is de-energized, and the power is dissipated through the load resistor. This process can be observed from the negative slope of the inductor current waveform. The output voltage was measured to be 50.5 V when the reading was taken by a multimeter. This is very close to 54 which (5) predicts. The 6.5% difference is due to nonideal effects and parasitic components which were not included in the development of (5). Fig. 19 shows the current waveforms of switches S_1 and S_2. It can be observed that experimental and simulation results agree with each other. Fig. 20 shows the transient response of the open-loop DI buck converter to a step change in the load resistance. The dynamic response is similar to that of a single-input buck converter. The variations of the

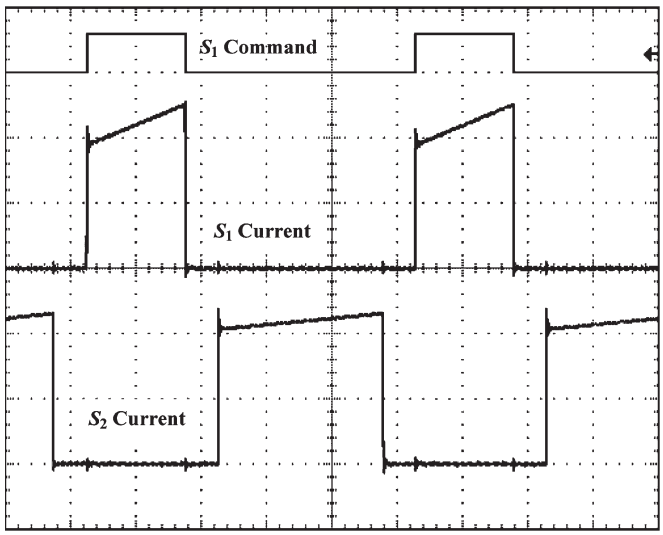

Fig. 19. Experimental current waveforms of the switches in a DI buck converter (current: 5 A/div and time: 4 μs/div).

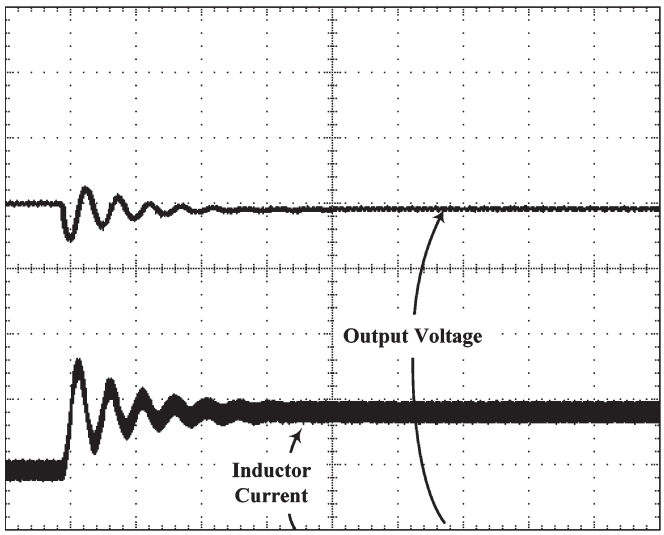

Fig. 20. Transient response of the DI buck converter to a step-down load change (voltage: 10 V/div, current: 10 A/div, and time: 1 ms/div).

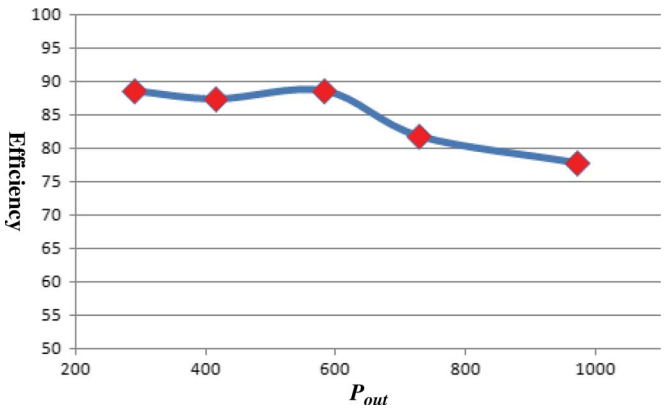

Fig. 21. Efficiency of the DI buck converter versus the output power.

efficiency of the DI buck converter versus the output power are shown in Fig. 21. The curve follows the efficiency curves of classic dc–dc converters.

VI. Conclusion

Three DI converters are developed in this paper using a SPTT switch as a building block. All of the proposed converters use only one inductor, which results in a reduced size and part count of the system. The proposed converters can be used in ultracapacitor enhancement of battery packs in automotive applications or hybridizing photovoltaic or fuel cell systems. Simulation and experimental results agree with the analytical results.

References

[1] Q. Mei, X. Zhen-lin, and W. Wu, "A novel multi-port dc–dc converter for hybrid renewable energy distributed generation systems connected to power grid," in *Proc. IEEE ICIT*, Chengdu, China, Apr. 2008, pp. 1–5.

[2] Y. M. Chen and Y. C. Liu, "Development of multi-port converters for hybrid wind–photovoltaic power system," in *Proc. IEEE Region 10 Int. Conf. Elect. Electron. Technol.*, Aug. 2001, vol. 2, pp. 804–808.

[3] Y. M. Chen, Y. C. Liu, S. C. Hung, and C. S. Cheng, "Multi-input inverter for grid-connected hybrid PV/wind power system," in *Proc. IEEE Trans. Power Electron.*, May 2007, vol. 22, pp. 1070–1077.

[4] Y. M. Chen, C. S. Cheng, and H. C. Wu, "Grid-connected hybrid PV/wind power generation system with improved dc bus voltage regulation strategy," in *Proc. IEEE APEC*, Mar. 2006, pp. 1088–1094.

[5] J. Sebastian, P. Villegas, M. M. Hernando, and S. Ollero, "High quality flyback power factor corrector based on a two input buck post-regulator," in *Proc. IEEE Appl. Power Electron. Conf.*, Feb. 23–27, 1997, vol. 1, pp. 288–294.

[6] C. C. Chan, "The state of the art of electric and hybrid vehicles," *Proc. IEEE*, vol. 90, no. 2, pp. 247–275, Feb. 2002.

[7] C. C. Chan, "The state of the art of electric, hybrid, and fuel cell vehicles," *Proc. IEEE*, vol. 95, no. 4, pp. 704–718, Apr. 2007.

[8] C. C. Chan, "An overview of electric vehicle technology," *Proc. IEEE*, vol. 81, no. 9, pp. 1202–1213, Sep. 1993.

[9] C. C. Chan and K. T. Chau, "An overview of power electronics in electric vehicles," *IEEE Trans. Ind. Electron.*, vol. 44, no. 1, pp. 3–13, Feb. 1997.

[10] M. K. C. Marwali, N. M. Maricar, and S. K. Shrestha, "Battery capacity tests evaluation for stand-alone photovoltaic systems," in *Proc. IEEE Power Eng. Soc. Winter Meeting*, Jan. 2000, vol. 1, pp. 540–545.

[11] M. Glavin and W. G. Hurley, "Battery management system for solar energy applications," in *Proc. IEEE Univ. Power Eng. Conf.*, Sep. 2006, vol. 1, pp. 79–83.

[12] H. Tao, A. Kotsopoulos, J. L. Duarte, and M. A. M. Hendrix, "Multi-input bidirectional dc–dc converter combining dc-link and magnetic-coupling for fuel cell systems," in *Conf. Rec. IEEE IAS Annu. Meeting*, Oct. 2–6, 2005, vol. 3, pp. 2021–2028.

[13] H. Tao, A. Kotsopoulos, J. L. Duarte, and M. A. M. Hendrix, "Family of multi-port bidirectional dc–dc converters," in *Proc. IEEE Elect. Power Appl.*, May 2006, vol. 153, pp. 451–458.

[14] Y. Chen, Y. Liu, F. Wu, and T. Wu, "Multi-input dc/dc converter based on the flux additivity," in *Conf. Rec. IEEE IAS Annu. Meeting*, 2001, pp. 1866–1873.

[15] Y. Chen, Y. Liu, and F. Wu, "Multi-input dc/dc converter based on the multiwinding transformer for renewable energy applications," *IEEE Trans. Ind. Appl.*, vol. 38, no. 4, pp. 1096–1104, Jul./Aug. 2002.

[16] Y. M. Chen, Y. C. Liu, and F. Y. Wu, "Multi-input converter with power factor correction, maximum power point tracking, and ripple-free input currents," *IEEE Trans. Power Electron.*, vol. 19, no. 3, pp. 631–639, May 2004.

[17] Y. M. Chen, Y. C. Liu, F. Y. Wu, and Y. E. Wu, "Multi-input converter with power factor correction and maximum power point tracking features," in *Proc. IEEE APEC*, Mar. 2002, vol. 1, pp. 490–496.

[18] A. D. Napoli, F. Caricchi, F. Crescimbini, O. Honorati, and E. Santini, "Testing of a new dc–dc converter topology for integrated wind-photovoltaic generating systems," in *Proc. IEEE 5th Eur. Conf. Power Electron. Appl.*, Sep. 1993, vol. 8, pp. 83–88.

[19] A. D. Napoli, F. Crescimbini, S. Rodo, and L. Solero, "Multiple input dc–dc power converter for fuel-cell powered hybrid vehicles," in *Proc. IEEE Power Electron. Spec. Conf.*, Jun. 2002, vol. 4, pp. 1685–1690.

[20] A. D. Napoli, F. Crescimbini, L. Solero, F. Carricchi, and F. G. Capponi, "Multiple-input dc–dc power converter for power-flow management in hybrid vehicles," in *Conf. Rec. IEEE IAS Annu. Meeting*, Oct. 2002, vol. 3, pp. 1578–1585.

[21] K. P. Yalamanchili, M. Ferdowsi, and K. Corzine, "New double-input dc–dc converters for automotive applications," in *Proc. IEEE Vehicular Power Populs. Conf.*, 2006, pp. 1–6.
[22] Y. M. Chen, Y. C. Liu, and S. H. Lin, "Double-input PWM dc/dc converter for high/low-voltage sources," *IEEE Trans. Ind. Electron.*, vol. 53, no. 5, pp. 1538–1545, Oct. 2006.
[23] P. Wood, *Switching Power Converters*. New York: Van Nostrand Reinhold, 1981, ch. 3.
[24] K. P. Yalamanchili, "Multi-input dc–dc converters for combined energy storage systems in hybrid electric vehicles," M.S. thesis, Univ. Missouri-Rolla, Rolla, Dec., 2006.
[25] N. D. Benavides and P. L. Chapman, "Power budgeting of a multiple-input buck-boost converter," *IEEE Trans. Power Electron.*, vol. 20, no. 6, pp. 1303–1309, Nov. 2005.
[26] B. G. Dobbs and P. L. Chapman, "A multiple-input dc–dc converter topology," *IEEE Power Electron. Lett.*, vol. 1, no. 1, pp. 6–9, Mar. 2003.
[27] N. D. Benavides, T. Esramand, and P. L. Chapman, "Ripple correlation control of a multiple-input dc–dc converter," in *Proc. IEEE Power Electron. Spec. Conf.*, 2005, pp. 160–164.
[28] A. Davoudi, J. Jatskevich, and P. L. Chapman, "Parametric average-value modeling of multiple-input buck converters," in *Proc. IEEE Can. Conf.*, Apr. 22–26, 2007, pp. 990–993.
[29] D. W. Hart, *Introduction to Power Electronics*. Englewood Cliffs, NJ: Prentice-Hall, 1997.

Karteek Gummi was born in Hyderabad, India, in 1984. He received the B.Sc. degree in electrical and electronics engineering from Osmania University, Hyderabad, in 2006 and the M.Sc. degree from the Missouri University of Science and Technology, Rolla (formerly University of Missouri-Rolla) in 2008, specializing in power electronics and power systems.

He began his career working for Bechtel Corporation in Houston, TX, in January 2008. In 2009, in order to get hands-on experience, he moved to a project in Tennessee to work on the construction of a nuclear power plant. He is currently working with the electrical engineering design group on that project.

Mehdi Ferdowsi (M'04) received the B.Sc. degree from the University of Tehran, Tehran, Iran, in 1997.

He is currently an Assistant Professor of electrical and computer engineering with the Missouri University of Science and Technology, Rolla. His research interests include energy storage systems, multi-input power electronic converters, projected cross point control, and plug-in hybrid electric vehicles.

Mr. Ferdowsi is a member of IEEE and an Associate Editor of the IEEE TRANSACTIONS ON POWER ELECTRONICS. He received the NSF CAREER award in 2007.